2D HILBERT-HUANG TRANSFORM

Jérémy Schmitt, Nelly Pustelnik, Pierre Borgnat, Patrick Flandrin

Laboratoire de Physique de l'Ecole Normale Suprieure de Lyon, CNRS and Université de Lyon, France
first.last@ens-lyon.fr

ABSTRACT

This paper presents a 2D transposition of the Hilbert-Huang Transform (HHT), an empirical data analysis method designed for studying instantaneous amplitudes and phases of non-stationary data. The principle is to adaptively decompose an image into oscillating parts called Intrinsic Mode Functions (IMFs) using an Empirical Mode Decomposition method (EMD), and them to perform Hilbert spectral analysis on the IMFs in order to recover local amplitudes and phases. For the decomposition step, we propose a new 2D mode decomposition method based on non-smooth convex optimization, while for the instantaneous spectral analysis, we use a 2D transposition of Hilbert spectral analysis called monogenic analysis, based on Riesz transform and allowing to extract instantaneous amplitudes, phases, and orientations. The resulting 2D-HHT is validated on simulated data.

Index Terms— Hilbert-Huang Transform, empirical mode decomposition, convex optimization, proximal algorithms, Riesz transform, monogenic analysis

1. INTRODUCTION

The 1D Hilbert-Huang Transform (1D-HHT), introduced by Huang *et al.* [1], is an empirical method for data analysis. Compared to usual time-frequency/time-scale method such as wavelet analysis or Wigner-Ville distribution, which aims at analysing non-linear and non-stationary signals, this method favours adaptivity.

Formally, the objective of 1D-HHT is to extract the instantaneous amplitudes $(\alpha^{(k)})_{1 \le k \le K}$ and phases $(\xi^{(k)})_{1 \le k \le K}$ from a signal $x \in \mathbb{R}^N$ built as a sum of elementary functions $(d^{(k)})_{1 \le k \le K}$ oscillating around zero, called Intrinsic Mode Functions (IMFs), and a trend $a^{(k)} \in \mathbb{R}^N$, i.e.,

$$x = a^{(k)} + \sum_{k=1}^{K} \underbrace{\alpha^{(k)} \cos \xi^{(k)}}_{d^{(k)}}.$$

To achieve this goal, the 1D-HHT consists in a two-step procedure combining (i) a decomposition step, whose objective is to extract the IMFs $(d^{(k)})_{1 \le k \le K}$ from the data x, with (ii) a Hilbert spectral analysis of each extracted IMF $d^{(k)}$

in order to estimate the instantaneous amplitudes $\alpha^{(k)}$ and phases $\xi^{(k)}$. Regarding the first step, an efficient decomposition procedure known as Empirical Mode Decomposition (EMD) has been proposed in [1]. It aims at sequentially extracting the IMF $d^{(k)}$ from a temporary trend $a^{(k-1)}$, defined as

$$\begin{cases} a^{(0)} = x, \\ (\forall k \in \{1, \ldots, K\}) \quad a^{(k-1)} = a^{(k)} + d^{(k)}, \end{cases}$$

through a sifting process that is based on the computation of a mean envelope of $a^{(k-1)}$ (mean of the upper and lower envelopes obtained by interpolating the maxima, resp. minima, of $a^{(k-1)}$).

The aim of this work is to propose the counterpart of the Hilbert-Huang transform for image analysis in order to decompose an image into elementary components and extract their instantaneous amplitudes, phases, and orientations. After a short review of related works in Section 2, we detail the proposed 2D-HHT method in Section 3. In Section 4, we illustrate the efficiency of the proposed method compared to the state-of-the art techniques on simulated data.

Notations We denote $\mathbf{y} = (\mathbf{y}_{n,m})_{1 \le n \le N_1, 1 \le m \le N_2} \in \mathbb{R}^{N_1 \times N_2}$ the matrix expression of an image whose size is $N_1 \times N_2$, the n-th row of the image $\mathbf{y}$ is denoted $\mathbf{y}_{n,\bullet} \in \mathbb{R}^{N_2}$, and $y = (y_n)_{1 \le n \le N} \in \mathbb{R}^N$ is the vector expression of $\mathbf{y}$, such that $N = N_1 \times N_2$.

2. RELATED WORKS

The Riesz-Laplace transform proposed in [2], which consists in a multiresolution 2D spectral analysis method, refers to the method with the closest goal to 2D-HHT. More precisely, this method aims at combining a two-dimensional wavelet transform with a monogenic analysis [3], which is based on Riesz analysis and appears to be a 2D extension of the Hilbert transform. The counterpart of using a wavelet framework is the lack of adaptivity and consequently this method is less suited for analysing non-stationary signals such as AM-FM signals. To build a genuine 2D-HHT method, a solution is to combine Felsberg and Sommer monogenic analysis [3] with a robust 2D-EMD. However, to the best of our knowledge, there is no such a solution in the literature.

Before detailing the proposed 2D-HHT, we will discuss the robustness of the existing EMD methods in order to highlight the necessity to propose a new robust 2D mode decomposition procedure. On the one hand, existing 2D-EMD methods are based on the sifting procedure whose main drawback is the lack of a rigorous mathematical definition, and consequently of convergence properties [4, 5, 6, 7, 8, 9]. On the other hand, efficient 1D mode decomposition procedures based on convex optimization have been recently proposed in order to get stronger mathematical guarantees [10, 11, 12]. For instance, [12] proposed a mathematical formalism for EMD based on a multicomponent proximal algorithm that combines the principle of texture-geometry decomposition [13, 14, 15] with some specific features of EMD: constraints on extrema in order to extract IMFs oscillating around zero, sequential aspect of EMD, or IMFs quasi-orthogonality. This methods appears to have better performance (in terms of extraction or convergence guarantees) than the other convex optimization procedures as discussed in [10, 11]. For this reason, we propose to extend this method to a 2D mode decomposition formalism and thus to combine it with a monogenic analysis in order to build a complete 2D-HHT.

3. PROPOSED 2D-HHT

3.1. 2D proximal mode decomposition

As discussed previously, the mode decomposition aims at splitting up the trend $a^{(k-1)}$ into a component having IMF properties (i.e. $d^{(k)}$), and a residual component, denoted $a^{(k)}$. To obtain such a decomposition we propose to solve

$$(a^{(k)}, d^{(k)}) \in \underset{a \in \mathbb{R}^N, d \in \mathbb{R}^N}{\text{Argmin}} \ \phi_k(a) + \psi_k(d) + \varphi_k(a, d; a^{(k-1)})$$

where ϕ_k and ψ_k denote convex, lower semi-continuous, and proper functions from $\mathbb{R}^N$ to $]-\infty, +\infty]$ that impose the trend and IMF behaviour to the components $a^{(k)}$ and $d^{(k)}$ respectively, while $\varphi_k(\cdot, \cdot; a^{(k-1)})$ denotes a convex, lower semi-continuous, proper function from $\mathbb{R}^N \times \mathbb{R}^N$ to $]-\infty, +\infty]$ that aims to model that $a^{(k-1)}$ is close to $a^{(k)} + d^{(k)}$.

The smoothness of the k-order trend is obtained by imposing a constraint on its total variation, i.e.,

$$\phi_k(a) = \eta^{(k)} \sum_{n=1}^{N_1} \sum_{m=1}^{N_2} \sqrt{|\mathbf{a}_{n-1,m} - \mathbf{a}_{n,m}|^2 + |\mathbf{a}_{n,m-1} - \mathbf{a}_{n,m}|^2}$$

with $\eta^{(k)} > 0$.

The tricky step in order to propose a 2D extension of the 1D proximal decomposition procedure [12] lies in the definition of the zero mean envelope constraint through the function ψ. Here we propose a "Pseudo 2D-EMD" approach, where lines, columns and diagonals extrema are separately constrained. For instance, the extrema-based constraint can be written for each row $n \in \{1, \ldots, N_1\}$, $\|R_n^{(k)} \mathbf{d}_{n,\bullet}\|_1$,

where $R_n^{(k)} \in \mathbb{R}^{N_2 \times N_2}$ denotes the linear combination of some elements of $\mathbf{d}_{n,\bullet}$ allowing to impose a zero mean envelope of the component $d^{(k)}$ (cf. [12] for the construction of $R_n^{(k)}$ that is similar due to the fact that a row $\mathbf{d}_{n,\bullet}$ behaves like a 1D signal). Considering the entire image, the constraint can be written $\|R^{(k)}d\|_1$ where $R^{(k)} = \text{diag}(R_1^{(k)}, \ldots, R_{N_1}^{(k)})$ is a block diagonal matrix in $\mathbb{R}^{N \times N}$, which is highly sparse. We apply the same type of constraint to the columns ($C^{(k)}$), the diagonals ($D^{(k)}$), and the anti-diagonals ($A^{(k)}$) of the image, leading to the penalization:

$$\psi_k(d) = \sum_{i=1}^{4} \lambda_i^{(k)} \|M_i^{(k)} d\|_1$$

where $M_1^{(k)} = R^{(k)}$, $M_2^{(k)} = C^{(k)}$, $M_3^{(k)} = D^{(k)}$, $M_4^{(k)} = A^{(k)}$ denote matrices in $\mathbb{R}^{N \times N}$.

As proposed in [16], the coupling term is chosen quadratic:

$$\varphi_k(a, d; a^{(k-1)}) = \|a + d - a^{(k-1)}\|^2.$$

The solution of the resulting minimization problem is obtained with Condat-Vũ primal-dual splitting algorithm [17] that allows to deal with linear operators and non-smooth functionals. The iterations are specified in Algorithm 1. For further details on the algorithmic solution and proximal tools, one may refer to [16].

3.2. Monogenic analysis of the extracted IMFs

Given a real-valued 1D signal y, the associated analytic signal $y_a(t)$, which by definition involves the signal itself and its Hilbert transform, can also be written under a polar form involving instantaneous phase and amplitude respectively denoted ξ and α such as: $y_a = y + j\mathcal{H}(y) = \alpha e^{j\xi}$. These two formulations allow to easily compute the instantaneous amplitude and the instantaneous phase as the absolute value of the analytic signal and its argument.

The Riesz transform is the natural 2D extension of the Hilbert transform [3]. The Riesz transform of a 2D signal $\mathbf{y}$ can be expressed as $\mathbf{y}_R = (\mathbf{y}^{(1)}, \mathbf{y}^{(2)}) = (h^{(1)} * \mathbf{y}, h^{(2)} * \mathbf{y})$, where the filters $(h^{(i)})_{1 \leq i \leq 2}$ are characterized by their 2D transfer functions $H_{\underline{\omega}}^{(i)} = -j\omega_i / \|\underline{\omega}\|$ with $\underline{\omega} = (\omega_1, \omega_2)$. On the other hand, the counterpart of the analytic signal in 2D is called the monogenic signal. It consists in the three-component signal defined by $\mathbf{y}_m = (\mathbf{y}, \mathbf{y}^{(1)}, \mathbf{y}^{(2)})$ [3]. In a similar way to the analytic signal, the monogenic signal enables to compute easily the local amplitude, phase, and orientation at each pixel through the relations, for every $(n, m) \in \{1, \ldots, N_1\} \times \{1, \ldots, N_2\}$,

$$\boldsymbol{\alpha}_{n,m} = \sqrt{\left(\mathbf{y}_{n,m}\right)^2 + \left(\mathbf{y}_{n,m}^{(1)}\right)^2 + \left(\mathbf{y}_{n,m}^{(2)}\right)^2} \quad (1)$$

$$\boldsymbol{\xi}_{n,m} = \arctan\left(\frac{\sqrt{\left(\mathbf{y}_{n,m}^{(1)}\right)^2 + \left(\mathbf{y}_{n,m}^{(2)}\right)^2}}{\mathbf{y}_{n,m}}\right) \quad (2)$$

$$\boldsymbol{\theta}_{n,m} = \arctan(\mathbf{y}_{n,m}^{(2)} / \mathbf{y}_{n,m}^{(1)}). \quad (3)$$

However, the estimation of the orientation proposed in (3) lacks of robustness because it does not take into account the orientation of neighbouring pixels. Unser *et al.* [2] derived an improved estimation based on a minimization procedure including a smoothness neighbourhood constraint. In our experiments, this robust technique is used.

3.3. 2D-HHT Algorithm

We now summarize the proposed 2D-HHT. In order to lighten the notations, we rewrite the total variation penalization as $\phi_k = \eta^{(k)}\|L \cdot \|_{2,1}$, with $L = [H^* V^*]^*$ where H and V denote the operators associated to the horizontal and vertical finite differences. We denote $M^{(k)} = \mathrm{diag}(M_1^{(k)}, M_2^{(k)}, M_3^{(k)}, M_4^{(k)})$. Parameters σ and τ are chosen so as to ensure the convergence of the algorithm, see [17] for details. The 2D-HHT method is summed up in Algorithm 1.

Algorithm 1 2D-HHT Algorithm

STEP 1 – **Initialization**
  Set $\mathbf{a}^{(0)} = \mathbf{x}$,
  Choose the number of IMFs K to be extracted,
  Set $k = 1$.
STEP 2 – **2D prox. mode decomp.** : extract $\mathbf{a}^{(k)}$ and $\mathbf{d}^{(k)}$ from $\mathbf{a}^{(k-1)}$.
  Compute $(M_i^{(k)})_{1 \le i \le 4}$ from $a^{(k-1)}$,
  Compute $\beta = 1 + \|\overline{M}^{(k)}\|^2$,
  Set $\sigma > 0$ and let $\tau = 0.9/(\sigma\beta + 2)$,
  Initialize $a^{[0]}$ and $d^{[0]}$ in $\mathbb{R}^N$,
  Initialize $y_0^{[\ell]}$ in $\mathbb{R}^{2N}$ and $y_i^{[\ell]} \in \mathbb{R}^N$ for $i = 1, \cdots, 4$.
  For $\ell = 0, 1, \cdots$
    $a^{[\ell+1]} = a^{[\ell]} - 2\tau(a^{[\ell]} + d^{[\ell]} - a^{(k-1)}) - \tau L^* y_0^{[\ell]}$
    $d^{[\ell+1]} = d^{[\ell]} - 2\tau(a^{[\ell]} + d^{[\ell]} - a^{(k-1)}) - \tau \sum_{i=1}^{4} M_{k,i}^* y_i^{[\ell]}$
    $y_0^{[\ell+1]} = \mathrm{prox}_{\sigma(\eta^{(k)}\|\cdot\|_{1,2})^*}(y_0^{[\ell]} + \sigma L(2a^{[\ell+1]} - a^{[\ell]}))$
    For $i = 1, \cdots, 4$
      $y_i^{[\ell+1]} = \mathrm{prox}_{\sigma(\lambda_i^{(k)}\|\cdot\|_1)^*}(y_i^{[\ell]} + \sigma M_{k,i}(2a^{[\ell+1]} - a^{[\ell]}))$
  Set $d^{(k)} = \lim_{\ell \to \infty} d^{[\ell]}$ and $a^{(k)} = \lim_{\ell \to \infty} a^{[\ell]}$.
STEP 3 – **Monogenic Analysis**
  Compute monogenic signal of $\mathbf{d}^{(k)}$: $\mathbf{d}_m^{(k)} = (\mathbf{d}^{(k)}, \mathbf{d}^{(k,1)}, \mathbf{d}^{(k,2)})$
  Compute local amplitude $\boldsymbol{\alpha}^{(k)}$, phase $\boldsymbol{\xi}^{(k)}$ and orientation $\boldsymbol{\theta}^{(k)}$
  using Eqs (1), (2), (3). ($\boldsymbol{\theta}^{(k)}$ can also be computed using Unser's improved method).
While $k < K$, set $k \leftarrow k + 1$ and return to STEP 2.

---

4. EXPERIMENTS

The image to be analyzed (Figure 1) consists in a sum of a trend and two localized texture components $\mathbf{x}^{(1)}$ and $\mathbf{x}^{(2)}$. The trend is formed with one rectangular patch and one ellipsoidal patch. The component $\mathbf{x}^{(1)}$ (resp. $\mathbf{x}^{(2)}$) models a modulated signal of central frequency $f_1 = 120/512$ (resp. $f_2 = 60/512$).

We apply the proposed 2D-HHT method to extract the two resulting IMFs and their local orientation estimates. In order to fairly compare with the state-of-the-art methods, we propose to replace the STEP 2 in Algorithm 1 with other decomposition methods such that Image Empirical Mode De-

composition [5], a natural 2D extension of 1D EMD based on 2D interpolation of extrema using thin-plate splines, and two texture-cartoon decomposition methods that are total variation and Gilles-Osher texture-geometry decomposition [14]. On the other hand we compare the extracted orientation with the results obtained from the Riesz-Laplace analysis proposed in [2]. Total variation decomposition consists in solving the optimization problem $\mathrm{Argmin}_{a \in \mathbb{R}^N} \|a - a^{(k-1)}\|_2^2 + \phi_k(a)$, where ϕ_k is the total variation constraint as defined in 3.1. Gilles-Osher is an iterative algorithm designed for solving Meyer's G-norm texture-cartoon decomposition model (we denote $\mu^{(k)}$ the texture regularization parameter and $\lambda^{(k)}$ the cartoon regularization parameter). We use the following optimal regularization parameters for our 2D-HHT : $\eta^{(1)} = 0.3$, $\lambda_i^{(1)} \equiv 0.3$, $\eta^{(2)} = 1$, $\lambda_i^{(2)} \equiv 0.1$. For Total Variation decomposition method, we use : $\eta^{(1)} = 70$ and $\eta^{(1)} = 100$. For Gilles-Osher method, we set $\mu^{(1)} = 10^4$, $\lambda^{(1)} = 10^3$, $\mu^{(2)} = 10$, and $\lambda^{(2)} = 10$. Results are shown on Figs 2 and 3.

First of all, our method provides a good separation of the different components. It has the expected behaviour of a 2D-HHT: the locally fastest oscillating components are extracted at each step of the decomposition, even if their frequencies are non stationary. Our proposed 2D-EMD method proved to perform better than previous 2D-EMD methods. For instance, the IEMD does not manage to separate at all the components $\mathbf{x}_1$ and $\mathbf{x}_2$. In comparison with other approaches like wavelet decomposition and texture-cartoon decomposition, the 2D-EMD approach provides more adaptivity and a better management of non-stationary signals. The Total Variation based approach does not give a good separation of the three oscillating components. Gilles-Osher solution is not suited for non-stationary signals: some of the slower part of the frequency modulated component $\mathbf{x}_2$ is on the 2nd IMF, while its faster part are localized on the first IMF. Finally, the Riesz-Laplace solution provides good results but this method is not adaptive and less suited for non-stationary signals. For instance, we can observe that some area of the same component but with different frequencies end up on different wavelet scales : here, the faster part of $\mathbf{x}_2$ is on the first scale, while the rest is on the second and third scale.

5. CONCLUSION

This paper proposes a complete 2D-HTT to extract local amplitudes, phases, and orientations of non-stationary images. This method is based on a 2D variational mode decomposition combined with a monogenic analysis using Riesz transform. This method has been tested on simulated data. In term of local orientation analysis, the proposed proved to be more efficient than existing 2D EMD methods and more adaptive than other decomposition approaches. In a future work, we will focus on the study of instantaneous frequencies considering the derivation of the local phase along the direction provided by the orientation.
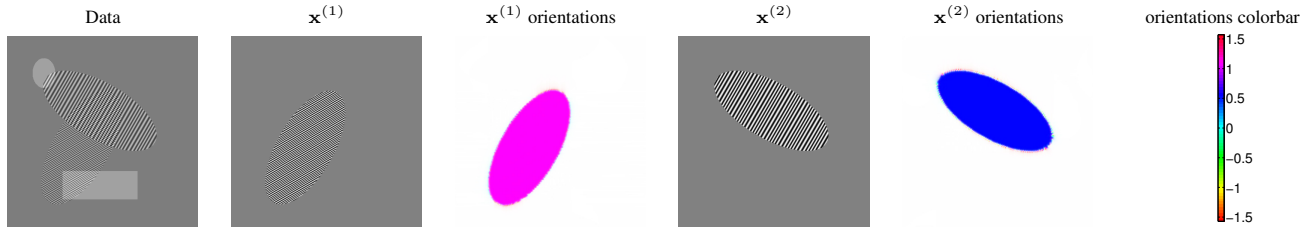
Fig. 1. Simulated data and its components : texture components $\mathbf{x}^{(1)}$, $\mathbf{x}^{(2)}$ and their local orientations.
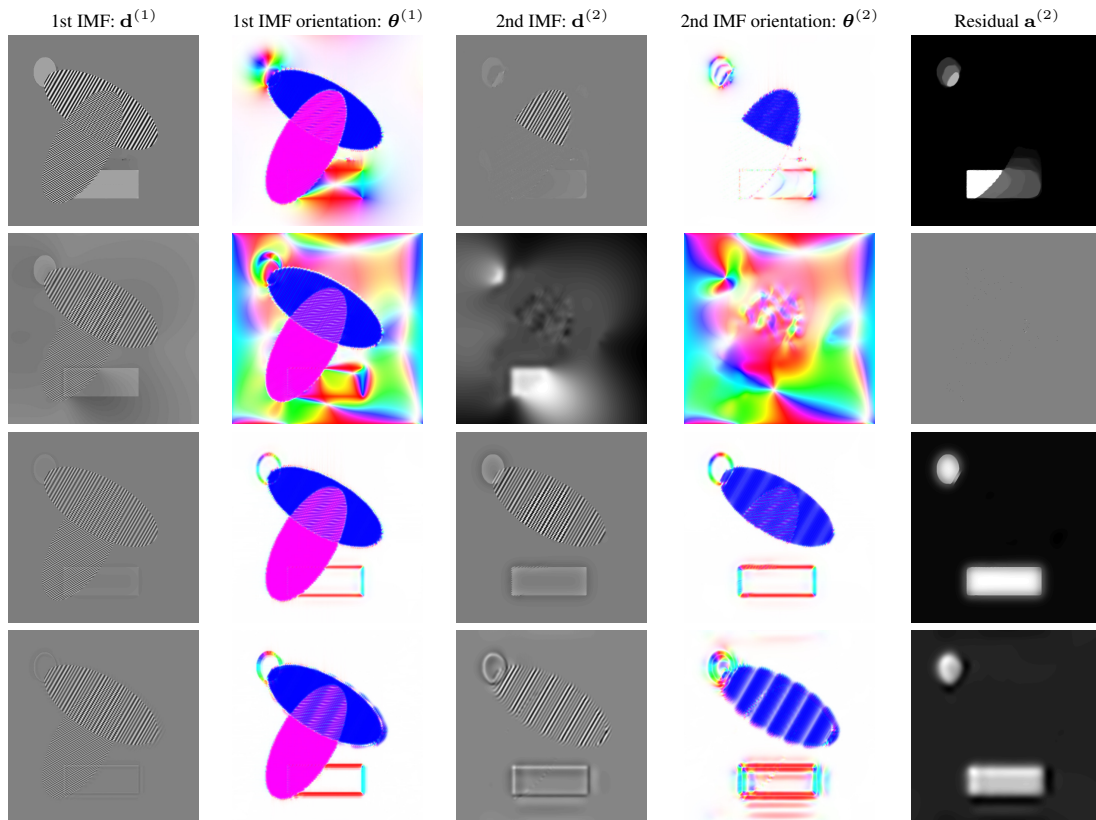

Fig. 2. Decomposition and local orientation of the simulated data presented in Fig. 1 obtained with different methods. 1st row: proposed solution, 2nd row: Image Empirical Mode Decomposition, 3rd row: Total Variation based decomposition, and 4th row: Gilles-Osher based decomposition. From the left to the right the columns present $\mathbf{d}^{(1)}$, $\boldsymbol{\theta}^{(1)}$, $\mathbf{d}^{(2)}$, $\boldsymbol{\theta}^{(2)}$, and $\mathbf{a}^{(2)}$.
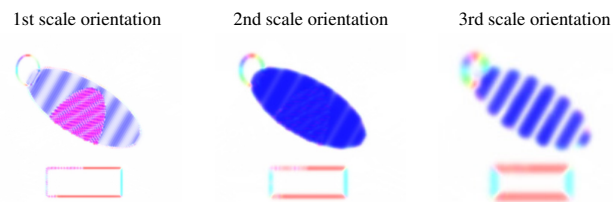

Fig. 3. Orientations estimated on 3 scales with Riesz-Laplace wavelet transform.

6. REFERENCES

[1] N.E. Huang, Z. Shen, S.R. Long, M.C. Wu, H. Shih, Q. Zheng, N.-C. Yen, C.C. Tung, and H.H. Liu, "The Empirical Mode Decomposition and the Hilbert spectrum for nonlinear and non stationary time series analysis," *Proc. R. Soc. A*, vol. 454, no. 2074, pp. 903–995, October 1998.

[2] M. Unser, D. Sage, and D. Van De Ville, "Multiresolution monogenic signal analysis using the Riesz-Laplace wavelet transform," *IEEE Trans. Image Process.*, vol. 18, no. 11, pp. 2402–2418, November 2009.

[3] M. Felsberg and G. Sommer, "The monogenic scale space : A unifying approach to phase-based image processing in scale-space," *J. Math. Imag. Vis.*, vol. 21, no. 1–2, pp. 5–26, July 2004.

[4] Z. Wu, N.E. Huang, and X. Chan, "The multidimensional Ensemble Empirical Mode Decomposition method," *Adv. Adapt. Data Anal.*, vol. 1, pp. 339–372, 2009.

[5] A. Linderhed, "Image Empirical Mode Decomposition: A new tool for image processing," *Adv. Adapt. Data Anal.*, vol. 1, no. 2, pp. 265–294, April 2009.

[6] J.-C. Nunes, Y. Bouaoune, E. Delechelle, O. Niang, and P. Bunel, "Image analysis by bidimensional Empirical Mode Decomposition," *Image Vis. Comput.*, vol. 21, no. 12, pp. 1019–1026, November 2003.

[7] C. Damerval, S. Meignen, and V. Perrier, "A fast algorithm for bidimensional EMD," *IEEE Signal Process. Lett.*, vol. 12, no. 10, pp. 701–705, October 2005.

[8] Y. Xu, B. Liu, J. Liu, and S. Riemenschneider, "Two-dimensional Empirical Mode Decomposition by finite elements," *Proc. R. Soc. A*, vol. 462, no. 2074, pp. 3081–3096, October 2006.

[9] B. Huang and A. Kunoth, "An optimization based Empirical Mode Decomposition scheme for images," *J. Comput. Appl. Math.*, vol. 240, pp. 174–183, March 2012.

[10] T. Oberlin, S. Meignan, and V. Perrier, "An alternative formulation for the Empirical Mode Decomposition," *IEEE Trans. Signal Process.*, vol. 60, no. 5, pp. 2236–2246, May 2012.

[11] T.Y. Hou, M.P. Yan, and Z. Wu, "A variant of the EMD method for multi-scale data," *Adv. Adapt. Data Anal.*, vol. 1, no. 4, pp. 483–516, October 2009.

[12] N. Pustelnik, P. Borgnat, and P. Flandrin, "A multicomponent proximal algorithm for Empirical Mode Decomposition," in *Proc. Eur. Sig. Proc. Conference*, August 2012, pp. 1880 – 1884.

[13] J.-F. Aujol, G. Gilboa, T. Chan, and S. Osher, "Structure-texture image decomposition - modeling, algorithms, and parameter selection," *Int. J. Comp. Vis.*, vol. 67, no. 1, pp. 111–136, April 2006.

[14] J. Gilles and S. Osher, "Bregman implementation of Meyer's G-norm for cartoon + textures decomposition," Tech. Rep., UCLA Computational and Applied Mathematics Reports, November 2011.

[15] J. Gilles, "Multiscale texture separation," *Multiscale Model. and Simul.*, vol. 10, no. 4, pp. 1409–1427, December 2012.

[16] P. L. Combettes and J.-C. Pesquet, "Proximal splitting methods in signal processing," in *Fixed-Point Algorithms for Inverse Problems in Science and Engineering*, H. H. Bauschke, R. Burachik, P. L. Combettes, V. Elser, D. R. Luke, and H. Wolkowicz, Eds., pp. 185–212. Springer-Verlag, New York, 2010.

[17] L. Condat, "A primal-dual splitting method for convex optimization involving Lipschitzian, proximable and linear composite terms," *J. Optim. Theory Appl.*, 2013, in press.